



Scale Model Tests of Multiple Barriers against Aircraft Impact: Part 1. Experimental Program and Test Results

Haruji Tsubota¹⁾, Norihide Koshika¹⁾, Jun Mizuno¹⁾, Mohsen Sanai²⁾, Brian Peterson²⁾,
Hideaki Saito³⁾ and Akira Imamura⁴⁾

1) *Kobori Research Complex, Inc., Japan*

2) *SRI International, USA*

3) *Tokyo Electric Power Co., Japan*

4) *Japan Nuclear Fuel Ltd., Japan*

ABSTRACT

The concept of a multiple barrier against aircraft impact has been recognized as an effective design method to mitigate damage to the critical components of nuclear-related structures. However, few experimental data have been collected to understand the phenomenology. This paper presents the results of scale model impact tests of multiple barriers. The impact loads to the second panels decrease markedly as the thickness of the first panel increases, thus confirming the effectiveness of the multiple barriers against aircraft impact.

1 INTRODUCTION

In current design of a nuclear-related structure against an aircraft impact, its outer walls and roofs are designed to protect the main facility inside the building. On the other hand, the authors propose the concept of multiple barriers, in which the critical equipment could be protected by the second wall and slab, while an aircraft is allowed to perforate through the first wall. If this concept is established, the thickness of outer walls and roofs could be decreased, and more reasonable and economical structural design would be possible. However, there is no established design method for multiple barriers at present.

As a first step for establishing the design method, this study intends to clarify the perforation phenomena caused by the global and local damage during a collision of an aircraft model onto reinforced concrete (RC) panels. For this purpose, impact tests using 1/7.5-scale models were performed, to assess the following items: 1) damage of the first RC panel, 2) scabbing concrete of the first RC panel, 3) residual velocity of the projectile after perforation, 4) impact load to the second panel.

2 IMPACT TEST METHODS

Impact test cases are shown in Table 1. The first RC panels are 1.5m square with 6, 8 and 10cm thicknesses. Reinforcement ratio is 0.47% each face each way, which is a current design requirement for barriers. In order to avoid damage near supports, boundary beams were placed around the RC panels. Figure 1 shows the reinforcement details of the RC panel for test MP-8-47 as a typical example. The first RC panel was supported by a reaction frame and was held in place by tensioned bolts at the four corners of the panel. The second panel was a 2m by 2m RC panel with 35cm-thick, and was suspended as a pendulum behind the first RC panel. The pendulum panel was instrumented with accelerometers to measure

the load produced by the debris from the aircraft model and the first RC panel. Prior to the main tests, an impact test onto a 16cm-thick panel was performed to estimate the dynamic strength of the projectile. The results of material tests of reinforcing bars and concrete used for the first RC panel and the pendulum are shown in Table 2.

The aircraft model was designed, with reference to the damage process of an actual aircraft during impact described in reference [1], so as to represent the characteristics of the engine and the fuselage without the wings. The collision response of the projectile could be characterized as follows: (i) the axial strength of the fuselage is small, and only the collided portion fractured brittlely; and (ii) the axial strength of the engine is relatively stronger than the fuselage, and it buckled from the front end. An overall schematic view of the aircraft model is shown in Figure 2. The fuselage consists of a 2mm-thick fiberglass cylinder and a high-density low-strength foam filler, and the engine consists of a 0.127mm-thick steel outer shell, a Hexcel honeycomb core, a lead tape attached to the outside and two 1.6mm-thick steel end plates. The mass distribution and the axial strength distribution of the manufactured projectile are shown in Figure 3. The axial strength distribution was derived separately for the fuselage and the engine using the following equation, based on the velocity reduction curve of the projectile (Figure 11) obtained from impact test results of the 16cm-thick panel.

$$Pc(x(t)) = m(x(t)) \cdot a(t), \quad \text{where } Pc(x(t)): \text{axial strength at location } x(t), \\ m(x(t)): \text{mass of undestroyed portion, and} \\ a(t): \text{acceleration of the undestroyed portion}$$

The gas propelled launcher facility located at Coral Hollow Experiment Site of SRI International was used to gradually accelerate the aircraft model to its impact velocity of 150 m/s. As shown in Figure 4, the major components of the facility include an acceleration cart, a two-rail support track, a high strength tow rope, a piston, a gas reservoir, a piston acceleration tube and a piston catcher tank. The aircraft model is attached to an acceleration cart, which in turn is mounted on 16.8m-long rail guides in the support track. A high strength tow rope is attached to the cart on one end and is attached to a piston on the other end. The piston is accelerated to the right using a reservoir of gas pressure while the cart is accelerated to the left. When the aircraft model has reached to the desired velocity, the cart is separated from the aircraft model which is allowed to collide onto the first panel after free flight.

For measurements, as shown in Figure 5, one accelerometer was mounted on the fuselage, and two were on the engine. The pendulum panel was instrumented with accelerometers whose layout is shown in Figure 6. Furthermore, high-speed cameras were placed perpendicular to the flight trajectory on the side of the first RC panel to record the impact of the projectile onto the RC panel. High-speed cameras were also on the backside of the first panel to observe the debris after the perforation.

3 IMPACT TEST RESULTS

The results of the tests are summarized in Table 3. Figure 7 shows the high-speed film sequence of the impact of the projectile onto the RC panel at test MP-10-47. The high-speed film sequence of first RC panel fracture and fragmentation of each test is shown in Figure 8. Furthermore, damaged front and back surfaces of each RC panel are shown in Figure 9, and the damaged fuselage and engine of test MP-8-47 are shown in Figure 10.

Figure 7 shows that the projectile collided with the middle of the RC panel, and only the collided portion of the projectile fractured at the nose. This damaging process corresponds well with the results of the actual aircraft impact test described in the reference [1]. Figure 10 indicates that the aircraft model was almost completely destroyed during the impact, most

of the fuselage turning into powder upon impact while only a small aft section of the fuselage remained intact. The engine remained intact, with the front portion being crushed by approximately 15cm for test MP-6-47 and MP-8-47, and 20cm for test MP-10-47. The results indicate that damage to the projectile increases with the thickness of the panel.

In Figure 8(a) of test MP-6-47, at 2ms after impact, the back surface of the RC panel started to crack at the grid of rebar of spacing 2.5cm. Thereafter, shear cones were formed and the projectile perforated through the panel. In Figure 8(b) for MP-8-47, cracks began to form approximately 2 ms after impact around the center of the back surface, with a grid 6 to 9 cm corresponding to the rebar spacing, and also in radial directions. After that, the cracks became magnified and the projectile perforated through the panel. In Figure 8(c) for MP-10-47, cracks became conspicuous approximately 4 ms after impact, in radial directions and along the perimeter of the slab. Even though the cracks became magnified thereafter, the projectile did not perforate through the RC panel.

Principal dimensions of the damaged area of the RC panels are summarized in Table 4. It shows that the hole in the thin panel is small and the damaged area is limited, while damage to the thick panels on the back surface tends to become large, leading to significant overall damage.

4 RESULTS OF MEASUREMENT

Velocity reduction curves of projectiles in each test case are shown in Figure 11. The velocity histories of the engine are obtained from on-board accelerometers, while the velocity histories of the fuselage were obtained from on-board accelerometers or high-speed films that shows the motion of the aft portion of the fuselage. The time 0 on the time axis denotes the instance at which the nose of the projectile collided with the first RC panel. According to the figure, velocity reduction curves of the fuselage and the engine tend to be similar in all test cases until the collision of the front end of the engine. Thereafter, the engine decelerates rapidly, separately from the fuselage. Comparing the results of each case, velocity reduction of the projectile tends to be larger for thicker panels.

Time histories of the impact load to the pendulum for each case are shown in Figure 12. The impact load was derived from the inertial force obtained by multiplying the measured accelerations, filtered by a low pass filter of 100 Hz, by the mass of the pendulum. In the figure, the impact load to a rigid panel derived from Muto's equation [1] is also shown for comparison. For all the test cases, the impact load was smaller than that obtained for the rigid panel, and the impact load to the second panel decreased drastically with increase in the panel thickness. The results indicate the possibility that multiple barriers would decrease the impact load exerted on the second panel.

5 CONCLUSION

In order to confirm the validity of multiple barriers against aircraft impact, scale model impact tests were performed using 1/7.5 models. The impact load to the second panel induced by an aircraft model that perforated through the first panel was derived from the experiment results. The experiment enabled quantitative assessment which showed a drastic decrease in the impact load to the second panel with increase in the thickness of the first RC panel, indicating the validity of the multiple barrier concept.

REFERENCES

1. Muto, K., Sugano, T., Tsubota, H., Koshika, N. et al, "Full-Scale Aircraft Impact Test for Evaluation of Impact Forces, Part1 and 2," 10th SMiRT, Vol. J, pp285-299, 1989

Table 1 Impact Test Cases

Test No.	First RC panel			Second panel
	Thickness (cm)	Reinforcement ratio ¹ (%)	Rebar spacing ¹	
MP-6-47	6	0.47	D3@25	Pendulum (RC 35cm-thick panel)
MP-8-47	8	0.47	D6@85	
MP-10-47	10	0.47	D6@68	

¹ Each face each way

Table 2 Material Test Results

(a) Reinforcement bar of first panel

Size	Yield strength (N/mm ²)	Tensile strength (N/mm ²)	Elongation (%)
D3	299	379	28.2
D6	346	493	28.8

(b) Concrete

	Test No.	Compressive strength (N/mm ²)
First panel	MP-6-47	31.4
	MP-8-47	38.2
	MP-10-47	34.8
Pendulum		38.6

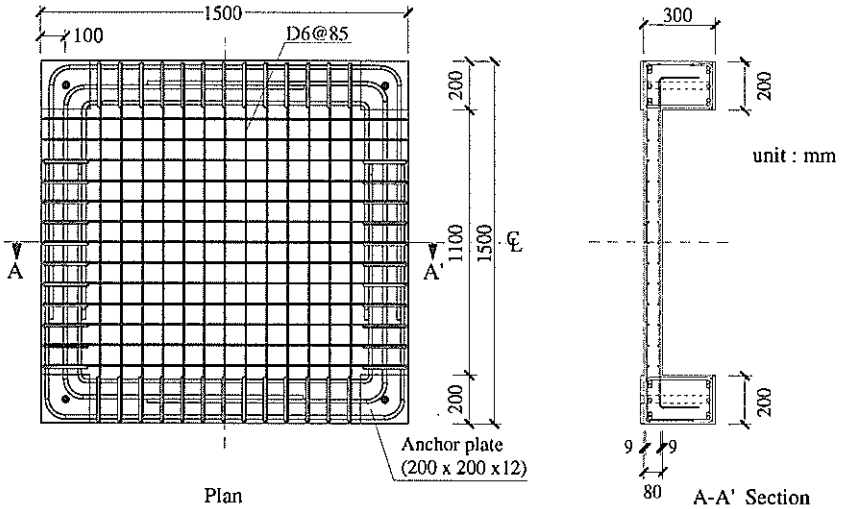
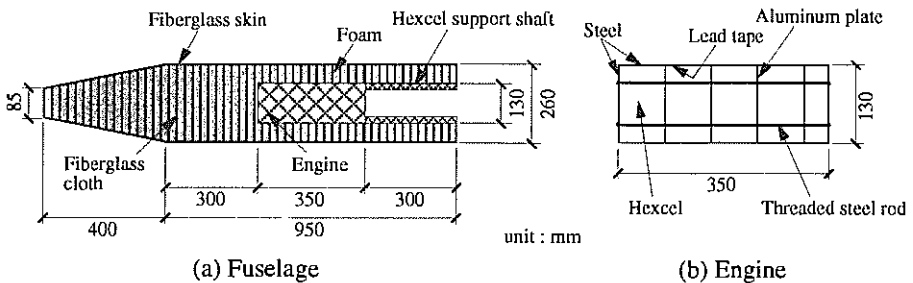


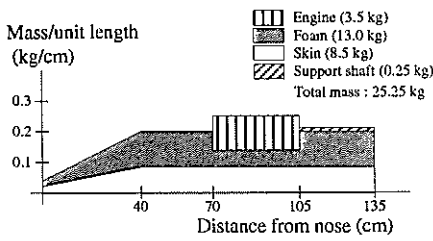
Figure 1 Dimension and Rebar Spacing of First Panel (MP-8-47)



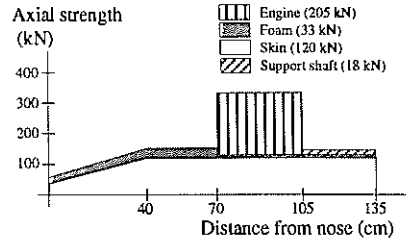
(a) Fuselage

(b) Engine

Figure 2 Schematic View of the Aircraft Model



(a) Mass distribution



(b) Strength distribution

Figure 3 Mass and Strength Distribution of Aircraft Model

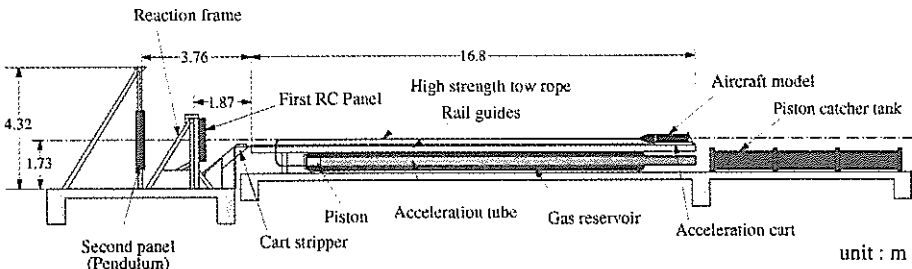


Figure 4 Gas Propelled Launcher Facility

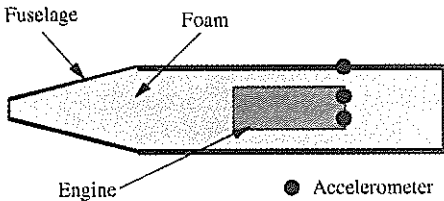


Figure 5 Location of Accelerometers on the Aircraft Model

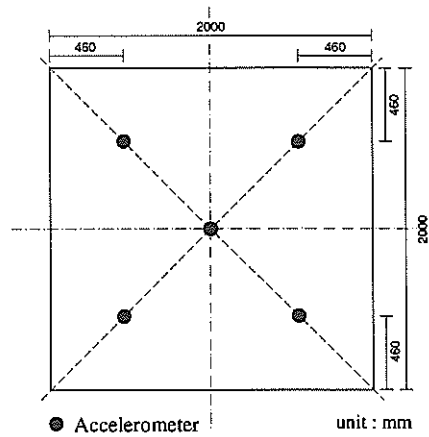


Figure 6 Layout of Accelerometers on the Back of Pendulum

Table 3 Summary of Impact Test Results

Test No.	Impact velocity (m/s)	Residual velocity (m/s)			Pendulum velocity (m/s)	Damage of first panel
		Fuselage	Engine	Scabbing concrete		
MP-6-47	142	110	80	80	90	Perforation
MP-8-47	149	70	- *	60	65	Perforation
MP-10-47	145	0	0	10	0	Penetration, Scabbing

* not recorded

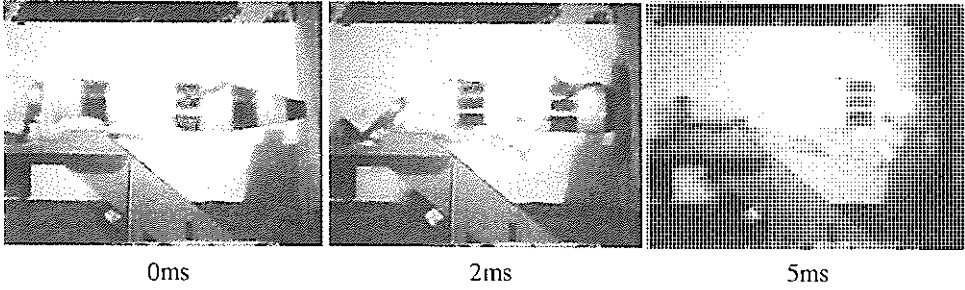
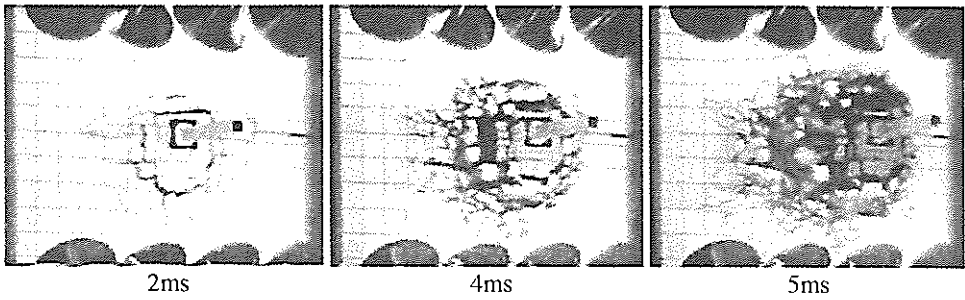
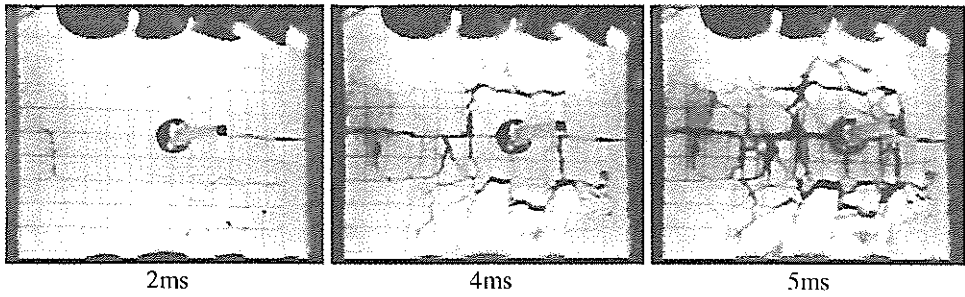


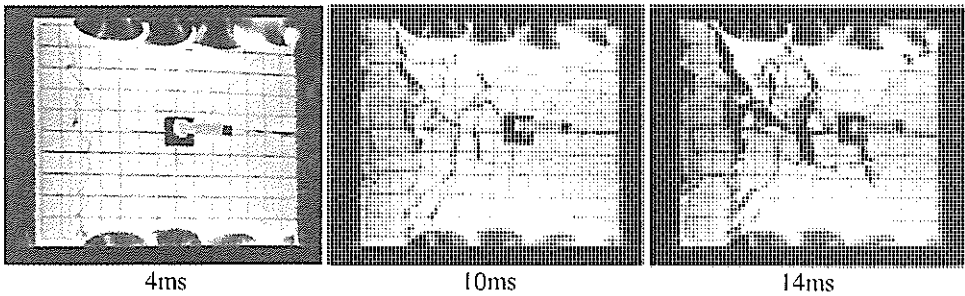
Figure 7 Hycam Film Sequence of MP-10-47 Impact



(a) Back of MP-6-47 panel

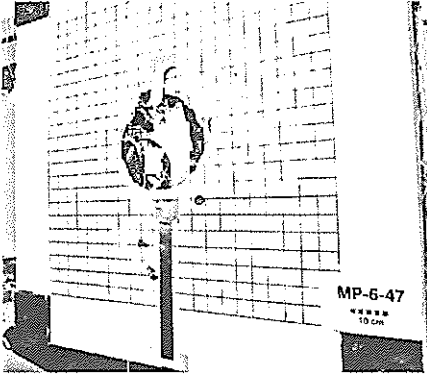


(b) Back of MP-8-47 panel

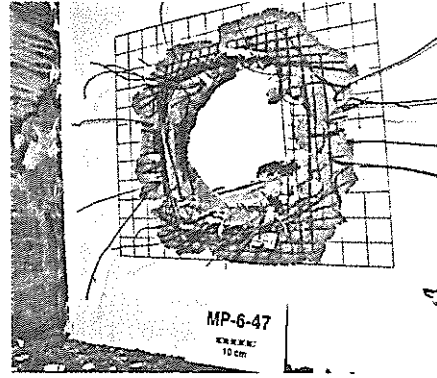


(c) Back of MP-10-47 panel

Figure 8 Hycam Film Sequence of First Panel Fracture and Fragmentation

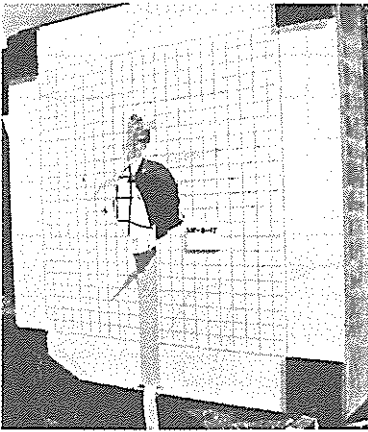


Front surface

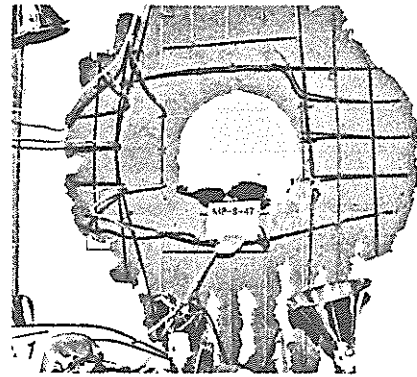


Back surface

(a) MP-6-47 panel

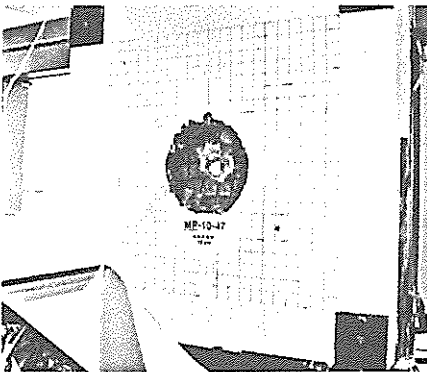


Front surface

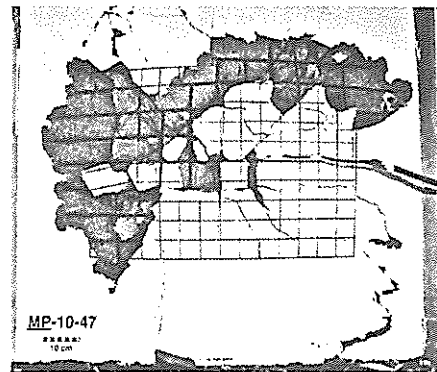


Back surface

(b) MP-8-47 panel



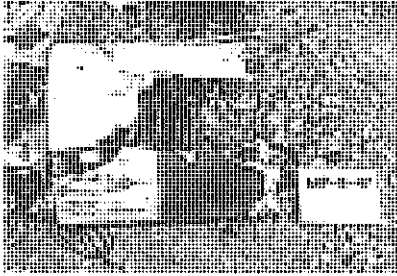
Front surface



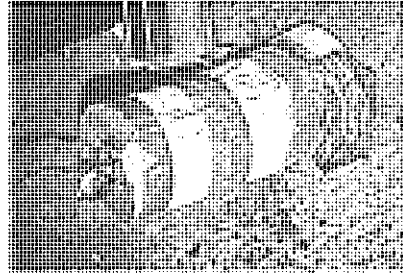
Back surface

(c) MP-10-47 panel

Figure 9 Damage to First Panel after Impact Test



(a) Fuselage

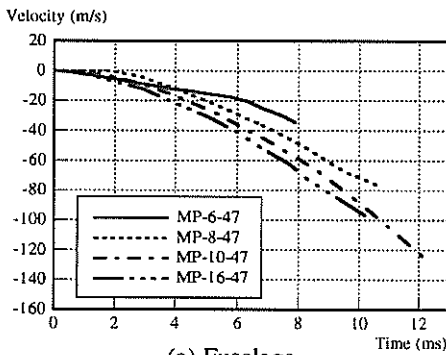


(b) Engine

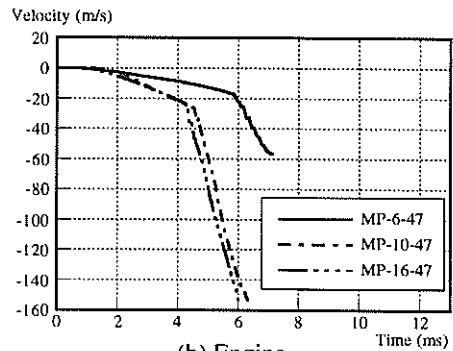
Figure 10 Damage of MP-8-47 Aircraft Model

Table 4 Damage Dimensions of First Panel

Test No.	Front surface		Backsurface
	Diameter of damaged area (cm)	Penetration depth (cm)	Damage area (width × height) (cm)
MP-6-47	33	Perforation	50 × 55
MP-8-47	30	Perforation	88 × 81
MP-10-47	38	8	103 × 103



(a) Fuselage



(b) Engine

Figure 11 Velocity Reduction Curve of Aircraft Model

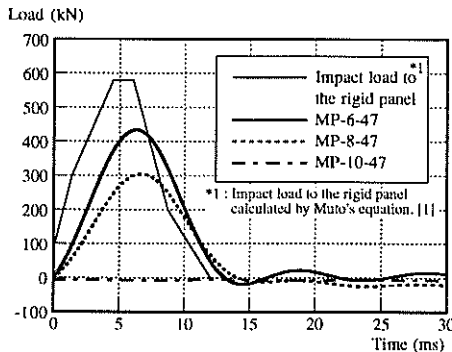


Figure 12 Impact Load to the Pendulum Panel after 100Hz Low Pass Filtering